

**ENERGY-STABLE RESIDUAL DISTRIBUTION
METHODS FOR SYSTEM OF SHALLOW WATER
EQUATIONS**

CHANG WEI SHYANG

UNIVERSITI SAINS MALAYSIA

2019

**ENERGY-STABLE RESIDUAL DISTRIBUTION METHODS FOR SYSTEM
OF SHALLOW WATER EQUATIONS**

by

CHANG WEI SHYANG

**Thesis submitted in fulfillment of the
requirements for the degree of
Doctor of Philosophy**

January 2019

ACKNOWLEDGEMENT

I thank God for His overflowed love and sustaining grace for my soul, His unsurpassed wisdom and soothing comfort for my mind, as well as His ultimate protection and abundant provisions for my body. There is none like Him.

I would like to extend my highest appreciation to my supervisor Assoc. Prof. Dr. Farzad Ismail for his beneficial guidances throughout my journey in this Ph.D. study. Besides being ever generous in sharing his vast knowledge in this field of study to his students, he is exceptionally understanding to their academical weaknesses and even personal struggles. I am also indebted to his insight for the direction of my study which have led me to the completion of this thesis.

I am also grateful to Universiti Sains Malaysia (USM) for financially supporting my Ph.D. candidature in USM through the Rancangan Latihan Kakitangan Akademik (RLKA) program, together with Skim Latihan Akademik IPTA (SLAI) of Education Ministry of Malaysia (KPM). I am tremendously thankful to both institutes for approving the extensions of candidature period I made to complete my research.

Many thanks to the dean of School of Aerospace Engineering, Prof. Ir. Dr. Mohd Zulkifly Abdullah for his kindness and support for my study, staff in the CATIA laboratory, Mrs. Rahayu Dorahim and others for helping me with technical issues of the computers, and even staff in the administrative office for dealing many documents of my research period extensions.

I would like to thank all my colleagues in the Aerospace CFD group, especially Dr. Hossain Chizari who spent considerable time with me to discuss about the research and the in-house code, as well as Mr. Vishal, Mr. Neoh, Mr. Siva and Ms. Mani who

have also exchanged thoughts and ideas with me over the span of this research.

I would like to also express my utmost thanks to my mother for her unwavering love, sacrifice in my upbringing and instilling the importance of knowledge in me. I also sincerely appreciate the accompaniments, supports and even laughters of both my brothers as well as my late father whom I respect. Last but not least, I would like to address my deepest gratitude towards my fiancée, Ms. Jasmine Farn for her love, faith, and smiles that enlighten my life.

TABLE OF CONTENTS

	Page
ACKNOWLEDGEMENT	ii
TABLE OF CONTENTS	iv
LIST OF TABLES	viii
LIST OF FIGURES	ix
LIST OF ABBREVIATIONS	xiii
LIST OF SYMBOLS	xiv
ABSTRAK	xvi
ABSTRACT	xvii
CHAPTER ONE: INTRODUCTION	
1.1 Background	1
1.2 Problem Statement	4
1.3 Research Objective	7
1.4 Scope of the Research	8
1.5 Thesis Outline	8
CHAPTER TWO: LITERATURE REVIEW	
2.1 Shallow Water Equations (SWE)	10
2.2 Finite Volume Method	14
2.2.1 Overview	14
2.2.2 Cell-vertex FVM	16
2.3 Residual Distribution Method	18
2.3.1 Overview	18
2.3.2 Properties of RD Methods	22
2.3.2(a) Positivity (\mathbb{P})	23

2.3.2(b)	Linearity Preserving (LP)	23
2.3.2(c)	Multidimensional Upwinding (MU)	24
2.3.3	Classic RD schemes	27
2.3.4	Stencil size of RD schemes	29
2.3.5	Minimal Susceptibility against Grid Distortion	31
2.3.6	Source term treatment	32
2.3.7	Flux Difference Method	33
2.4	Entropy Control	34
2.4.1	Overview	34
2.4.2	Entropy Conservation	38
2.4.3	Entropy Stability	39
2.4.4	Entropy Consistency	41
2.4.5	2D Entropy Stable FVM scheme	41
2.5	Numerical Methods for SWE	43
2.5.1	Well-balancedness property	43
2.5.2	Energy control	45
2.6	Summary	46
CHAPTER THREE: SCALAR EQUATIONS		
3.1	Introduction	47
3.2	Flux Difference RD Methods	50
3.2.1	Isotropic Signals	50
3.2.2	Artificial Signals	51
3.2.3	Time Integration	54
3.3	Condition for Positivity	56
3.4	Grid Skewness Variation	59
3.5	Von Neumann Stability Analysis	60

3.6	Order of Accuracy Analysis	66
3.6.1	Truncation Error	66
3.6.2	Formal Order of Accuracy of Flux Difference Approach on Right Running Grid	67
3.6.2(a)	Isotropic Signals	68
3.6.2(b)	Artificial Signals	70
3.6.3	First Order Scheme	72
3.6.4	Second and Higher Order Schemes	72
3.7	Implementation	73

CHAPTER FOUR: NUMERICAL SOLUTIONS OF SYSTEM OF SHALLOW WATER EQUATIONS

4.1	Overview	76
4.2	Energy-conserved RD for Shallow Water Equations	77
4.2.1	Well-balanced and Energy-Conserved RD for Non-homogeneous SWE	84
4.3	Role of artificial signals towards energy-stability	89
4.4	Achieving energy stability	92
4.4.1	Well-balanced and Energy-Stable RD for Non-homogeneous SWE	95
4.5	Energy-stable RD Approach for SWE	96
4.5.1	First order scheme with positivity property	96
4.5.2	Second order schemes with linear preserving property	97
4.5.2(a)	Baseline approach	97
4.5.2(b)	Alternative approach	98
4.5.3	Second order method with limiters	100
4.6	Time Integration	101
4.7	Grid generation and randomization	102
4.8	Boundary Conditions	103

CHAPTER FIVE: RESULTS AND DISCUSSION

5.1	The 2D scalar equations	105
5.1.1	Numerical stable range of CFL number	105
5.1.2	Order of Accuracy - Linear Advection	108
5.1.3	Monotone property - Shock Tree	116
5.2	The 2D Homogeneous Shallow Water Equations	118
5.2.1	Vortex Advection	119
5.2.2	Oblique Hydraulic Jump	121
5.2.3	Stoker's Dam Break	128
5.3	The 2D Non-homogeneous Shallow Water Equations	131
5.3.1	Lake at Rest	131
5.3.2	Sub-critical steady flow with a bump	134

CHAPTER SIX: CONCLUSION

6.1	Summary	139
6.2	Concluding Remarks	140
6.3	Future Works	142

REFERENCES	143
-------------------	------------

APPENDICES

Appendix A: Median-dual area of FV method

LIST OF PUBLICATIONS

LIST OF TABLES

		Page
Table 3.1	Classic RD schemes recovery with artificial signals.	55
Table 3.2	Range of Q and s considered in the analyses	60
Table 3.3	The amplification factor, $ \delta $ for N and LDA schemes.	65
Table 3.4	TE coefficients for different order of normal derivatives for first order classic RD methods.	67
Table 3.5	TE coefficients for different order of normal derivatives for higher order classic RD methods.	67
Table 5.1	Upper limit of ν from Von Neumann Analysis	107
Table 5.2	Summary of accuracy analysis of ESRD in comparison with various schemes for vortex advection	125
Table 5.3	Norm of the errors on water heights and u, v velocities at $t = 0.15$.	133

LIST OF FIGURES

		Page
Figure 2.1	Some notations for SWE.	13
Figure 2.2	The first order finite volume cell vertex diagram.	17
Figure 2.2(a)	Voronoi cell area of point 0 and the normal of each edge	17
Figure 2.2(b)	Net flux along edge i	17
Figure 2.3	The second order finite volume cell vertex stencil diagram.	18
Figure 2.4	Signal directions and median-dual area of a point.	22
Figure 2.4(a)	Signals from every neighbouring cells	22
Figure 2.4(b)	Median-dual area of a node	22
Figure 2.5	The inward normals of an element.	26
Figure 2.6	The 1-target and 2-target cells.	26
Figure 2.6(a)	1-target cell	26
Figure 2.6(b)	2-target cell	26
Figure 2.7	The stencil for isotropic grid for different upwind methods.	30
Figure 2.7(a)	N	30
Figure 2.7(b)	Upwind FVM 1 st	30
Figure 2.7(c)	LDA	30
Figure 2.7(d)	Upwind FVM 2 nd	30
Figure 2.8	The stencil for isotropic grid for different central methods.	31
Figure 2.8(a)	LxF	31
Figure 2.8(b)	Central FVM 1 st	31
Figure 2.8(c)	LxW	31
Figure 2.8(d)	Central FVM 2 nd	31
Figure 2.9	Control volume for entropy generation. Cell domain is shown by thick lines and shaded areas.	38
Figure 2.9(a)	Finite Volume Method	38

Figure 2.9(b)	Residual Distribution	38
Figure 2.10	A sample median-dual edge with normal and tangential velocities (q, r) in an arbitrary grid.	42
Figure 3.1	Residual distributed over triangular element.	48
Figure 3.2	Dual median area of a point (A_p is the shaded area)	56
Figure 3.3	Right-running grid topology. The characteristic line is $y = \frac{b}{a}x$	60
Figure 3.4	Visualization of elements with different skewness.	61
Figure 3.4(a)	$Q = 0.3$	61
Figure 3.4(b)	$Q = 0.6$	61
Figure 3.4(c)	$Q = 0.9$	61
Figure 3.5	Right-running grid terminology for stability analysis	64
Figure 3.6	The CFL condition for RD.	65
Figure 3.7	Flowchart of the in-house C++ code.	74
Figure 4.1	The general residual distribution scheme diagram.	79
Figure 4.1(a)	Neighbouring cells in Ψ that contribute their residuals to point 0	79
Figure 4.2	Arbitrary triangle with three node-pairs to mark different edges.	81
Figure 4.3	Isotropic and Artificial signals going to point i	92
Figure 4.4	Minimum distance, r_{\min} and shaded area for possible destination of shifted points after randomisation.	103
Figure 4.5	Solid wall boundary condition for RD.	104
Figure 5.1	Amplification factor plots at the border of stable(left)-unstable(right) CFL numbers.	106
Figure 5.1(a)	N scheme, $\nu = 3.0$	106
Figure 5.1(b)	N scheme, $\nu = 3.01$	106
Figure 5.1(c)	LDA, $\nu = 3.0$	106
Figure 5.1(d)	LDA, $\nu = 3.01$	106
Figure 5.1(e)	Baseline 1 st order, $\nu = 0.2$	106
Figure 5.1(f)	Baseline 1 st order, $\nu = 0.21$	106

Figure 5.1(g)	Positive 1 st order, $\nu = 2.0$	106
Figure 5.1(h)	Positive 1 st order, $\nu = 2.05$	106
Figure 5.1(i)	2 nd order, $\nu = 0.3$	106
Figure 5.1(j)	2 nd order, $\nu = 0.35$	106
Figure 5.2	Analytical order of accuracy for varying the skewness in right running grid at different ω_f .	110
Figure 5.2(a)	$\omega_f = 1$	110
Figure 5.2(b)	$\omega_f = 4$	110
Figure 5.2(c)	$\omega_f = 8$	110
Figure 5.3	Numerical order of accuracy for various the skewness in right running grid for $\omega_f = 1$.	111
Figure 5.4	Analytical truncation error in logarithmic scale for all the skewness in right running grid at different ω_f .	112
Figure 5.4(a)	$\omega_f = 1$	112
Figure 5.4(b)	$\omega_f = 4$	112
Figure 5.4(c)	$\omega_f = 8$	112
Figure 5.5	Truncation error (analytical) versus the grid distance in logarithmic scale for the linear case $Q = 0.7$ in the right running grid.	113
Figure 5.6(a)	N	114
Figure 5.6(b)	1 st order	114
Figure 5.5	u velocity contours for steady state linear advection test case	115
Figure 5.5(c)	LDA	115
Figure 5.5(d)	2 nd order	115
Figure 5.6	L2 errors residual plots against number of iterations for different RD schemes for steady linear advection test case at $\omega_f = 1$ and $Q = 0.4$	116
Figure 5.7	Cross section of different schemes for shock tree problem	117
Figure 5.8	Isotropic grids used for Vortex advection problem	120

Figure 5.9	Water height profiles across the vortex at streamline direction for various schemes on $[200 \times 200]$ grid	122
Figure 5.10	u velocity profiles across the vortex at streamline direction for various schemes on $[200 \times 200]$ grid	123
Figure 5.11	L2 errors of water height, h versus the grid distance in logarithmic scale for vortex advection	124
Figure 5.12	Exact solutions and 70% randomised isotropic grid used.	127
Figure 5.13	Water height profiles across $y = 0.85$ for various schemes on grid with 70% randomisation for oblique hydraulic jump.	129
Figure 5.14	Convergence errors residual plots of various schemes for oblique hydraulic jump.	130
Figure 5.15	Water height profiles across $y = 0.5$ of various schemes for dam break problem.	132
Figure 5.16	Exact total water height profile and the bottom topography for sub-critical flow with a bump.	135
Figure 5.17	Total water height profile above the bump for various schemes on $[200 \times 50]$ grid.	136
Figure 5.18	L2 errors of water height, h versus the grid distance in logarithmic scale for sub-critical flow with a bump.	137
Figure A.1	The first order finite volume cell vertex diagram.	155
Figure A.1(a)	Median-dual cell area of point 0 and the normal of each edge	155
Figure A.1(b)	Net flux along edge i	155

LIST OF ABBREVIATIONS

CFD	Computational Fluid Dynamics
PDE	Partial Differential Equation
FDM	Finite Difference Method
FVM	Finite Volume Method
FEM	Finite Element Method
RD	Residual Distribution
SEM	Spectral Element Method
FPM	Finite Point Method
SWE	Shallow Water Equations
ESRD	Energy(Entropy) Stable Residual Distribution
ESFV	Energy(Entropy) Stable Finite Volume
1D	One-Dimensional
2D	Two-Dimensional
3D	Three-Dimensional
SUPG	Streamline-Upwind Petrov-Galerkin
PSI	Positive Streamwise Invariant
LED	Local Extremum Diminishing
N	Narrow-scheme
LxF	Lax-Friedrichs
LDA	Low Diffusion Advection
LxW	Lax-Wendroff
LMT	Limited
RR	Right-Running
CFL	Courant–Friedrichs–Lewy
OoA	Order of Accuracy
TE	Truncation Error
WB	Well-Balanced

LIST OF SYMBOLS

\mathbf{u}	SWE Conservative variables
$\vec{\mathbf{f}}$	SWE flux vector
$\vec{\mathbf{s}}$	SWE source term
(\mathbf{f}, \mathbf{g})	SWE flux components
Fr	Froude number
g	Gravitational field strength
u	Scalar conservative variables
\vec{f}	Scalar flux vector
(f, g)	Scalar flux components
s	Scalar source term
A_p	Nodal median-dual area
$\hat{\mathbf{n}}_e$	Outwards normal of the edge e
\hat{l}_e	length of the edge e
$\phi^{\mathbb{E}}$	Scalar total residual of an element
$\Phi^{\mathbb{E}}$	SWE total residual of an element
$\zeta_i^{\mathbb{E}}$	The portion of signal distributed to node i in element \mathbb{E}
Ψ	Set of neighbouring cells of a node
\mathbb{E}	Element/Cell
$l_{\mathbb{E}}$	Element/cell size
$\vec{\lambda}$	Scalar characteristic vector
\vec{n}_i	Scaled normal vector of the edge opposite of node i
k_i	Scalar Jacobian scaled with length for edge i
k_i^{\pm}	Scalar positive or negative Jacobian scaled with length for edge i
E	Entropy (Energy) function
\vec{F}	Entropy (Energy) flux vector
(F, G)	Entropy (Energy) fluxes
\vec{S}	Entropy (Energy) source term
\dot{E}	Entropy generation (Energy dissipation) rate

\mathbf{v}	Symetrizing entropy (energy) variables
\mathbf{R}	Right eigenvector matrix
$\mathbf{\Lambda}$	Diagonal eigenvalue matrix
\mathbf{L}	Left eigenvector matrix
\mathbf{S}	Diagonal scaling matrix
Δt	Iteration time step size
σ	Stretching paramter
Q	Grid skewness
$ \delta $	Amplification factor
ν	CFL number
ψ	Blending parameter
ω_f	Wave frequency

KAEDAH TENAGA-STABIL PENGEDARAN SISA UNTUK SISTEM PERSAMAAN AIR CETEK

ABSTRAK

Satu kaedah Pengedaran Sisa Tenaga-Stabil (ESRD) yang canggih telah diperluaskan untuk sistem Persamaan Air Cetek (SWE) sebagai satu penambahbaikan daripada kaedah isipadu (ESFV) sehingga tenaga-stabil untuk mewarisi ciri multidimensi, kepekaan yang minimum terhadap gangguan grid dan keupayaan untuk mencapai urutan ketepatan yang lebih tinggi dengan stensil yang lebih kecil. ESRD mengenakan kawalan tenaga secara serentak dengan pengiraan pembolehubah utama melalui pemetaan pembolehubah konservatif utama kepada pembolehubah tenaga. Keadaan pemuliharaan tenaga dan keadaan tenaga-stabil dicapai melalui reka bentuk isyarat isotropik dan isyarat buatan masing-masing. Hanya kaedah yang jelas telah dikaji untuk mengekalkan keberkesanan kos skema ini. Sumbangan utama kajian ini ialah pendiskretan istilah sumber untuk mencapai sifat keseimbangan berangka. Kesan variasi kecondongan grid atas ketepatan dan kestabilan ESRD diperiksa berdasarkan analisis skalar. Parameter-parameter kebebasan telah diselidikan untuk memperoleh sifat positif (skim urutan pertama) dan sifat pemeliharaan linear (skim urutan kedua). Skim terhad bukan linear juga direka dengan pencampuran skim urutan pertama dan kedua. Berbeza dengan ESFV, ESRD telah menunjukkan kebolehan untuk mengekalkan urutan ketepatan walaupun pada grid segi tiga dengan perawakan yang tinggi. Keseimbangan skim yang dicadangkan telah disahkan dan urutan ketepatan versi skim yang seimbang dipelihara.

ENERGY-STABLE RESIDUAL DISTRIBUTION METHODS FOR SYSTEM OF SHALLOW WATER EQUATIONS

ABSTRACT

A state-of-the-art Energy-Stable Residual Distribution (ESRD) method is expanded for a system of Shallow Water Equations (SWE) as an improvement over the finite volume counterpart (ESFV) for inheriting multi-dimensional feature, minimal sensitivity to grid distortions and the ability to achieve higher order accuracy with smaller stencil. ESRD imposes energy control simultaneously with the computation of the main variables through the mapping of primary conservative variables to energy variables. The energy conservation and energy stable conditions are achieved via the design of isotropic signals and artificial signals respectively. To preserve the cost-effectiveness of the scheme, the work is limited to only full explicit approach. The main contribution of this work is the source term discretisation which is designed to achieve numerical well-balancedness property. The effects of grid skewness variations on the order of accuracy and stability of ESRD were examined based on scalar analyses. Different degrees of freedom were manipulated to achieve positivity (first order scheme) and linear preserving (second order scheme) properties. A non-linear limited scheme is also constructed with the blending of the first and second order schemes. Unlike ESFV, ESRD demonstrates its ability to preserve the order of accuracy even on high randomized triangular grids. The well-balancedness of the proposed scheme was validated numerically and the order of accuracy of the well-balanced version of the schemes are still preserved.

CHAPTER ONE

INTRODUCTION

1.1 Background

Within the context of scientific studies of fluids, there are generally three main branches to obtain solutions of fluid dynamics, namely analytical, numerical and experimental means. By using established mathematical models of fluid flow, the exact solutions can be formulated through analytical approach. However, the governing equations usually do not have closed solutions with the exception of specific simplification on the flow conditions and geometries which renders the applications of this approach to be very limited. On the other hand, the experimental approach involves physical re-enactment of the actual fluid flow conditions. Although the experiments can be scaled based on certain dimensionless parameters to simplify them, the results of the tests are still susceptible to numerous experimental errors as well as the limitations of measuring devices. Besides, the experiments are usually relatively more expensive, time-consuming and not economical to be used for the whole engineering design process.

The numerical approach, categorized as Computational Fluid Dynamics (CFD), has great potential, robustness [Petridis, Knight, & Edwards, 1991] and capability to produce reliable fluid dynamics solutions. The main driving force behind this approach is the rapid development of the hardware computing capacity and efficiency. Higher level of sophisticated fluid problems can also be solved within acceptable time frame via CFD, especially with the introduction of high performing computers and parallel

computing.

Similar to the analytical approach, CFD uses mathematical models to represent the fluid flow physics and attempts to solve the governing equations which are usually in the form of Partial Differential Equations (PDE). However, these equations are solved through a series of numerical algorithms, which is a form of estimation. The computations are performed to determine values at discrete points in the domain. Hence, it is obvious that CFD suffers from numerical errors which are due to the type of algorithm employed as well as the machine errors from the discretisation of data by the computer. The rapid growth of computing memory capacity has reduced the machine errors to a minimal level, which leaves the major contribution of the numerical errors to the choice of numerical techniques employed. Hence, it is crucial to invest in the researches regarding the numerical methods to propel CFD to the next stage and reach its full potential.

In general, numerical methods can be classified into Finite-Difference Method (FDM), Finite-Volume Method (FVM), Finite-Element Method (FEM), Residual Distribution (RD), Spectral Element Method (SEM) and even meshless methods such as Finite Point Method (FPM) [T. J. Chung, 2002]. Being the earliest introduced method, FDM is the simplest and most straightforward approach to approximate PDEs, which is also commonly used by academicians to introduce numerical methods to students. FDM only uses nodal values in the calculations of the derivative terms in the governing equations.

On the other hand, FVM considers the computational domain as small discrete cells

and utilizes the Divergence/Green's theorem (depending on the dimensions) to evaluate the divergence terms in the PDEs as fluxes at the cells' boundaries. Conservation is easily attained in FVM by ensuring the total fluxes entering and leaving the cells to be equal, which is the main feature that attracts many CFD packages to opt FVM over other methods [T. J. Chung, 2002].

Another alternative, FEM has received vast popularity in applications such as structural analysis, heat transfer problems and even fluid flow as well. In short, the computational domain for FEM is also discretised into small cell/element and by using Galerkin method analogy, weighting functions are introduced to the integral form of the PDEs which are then deemed as residual. The weighting functions are set up as polynomial approximate functions in order to minimize the residual errors.

The RD method is relatively new compared to the three aforementioned methods and it can be seen as a hybrid between FVM and FEM but with its own distinct properties. Although RD has its own advantages, there are still numerous unresolved issues which are the main factors that it is not widely used yet [Deconinck, Sermeus, & Abgrall, 2000].

The interesting category of meshless methods is considered as an unique extension from FDM as both estimates the differential form of the governing equations. The meshless methods have been tested on some simple smooth problems with good results but potential issues with shock are foreseen since they focus on the differential equations [T. J. Chung, 2002].

1.2 Problem Statement

The idea of entropy control in numerical algorithm can be traced back to [Harten, 1983] who first introduced the connection of entropy with the governing equations of fluid dynamics and [Tadmor, 1987b] on the numerical algorithms that enforce entropy control. The weak solutions of the conservation laws of mass, momentum and energy are not necessarily unique and thus require additional constraint(s). One good choice of this criterion is the Second Law of Thermodynamics which states that the total entropy for a closed physical system can either remain constant for a reversible process and is always increasing for an irreversible process.

Tadmor, (1987a) in his works of symmetrizing hyperbolic systems of conservation laws, has proposed a convex entropy function which in turn was utilized for entropy control. However, Tadmor's approach did not attract much attention due to its high computational cost. Consequently, most numerical schemes only follow some loose entropy conditions upon the encountering of a shock without any explicit mechanism to preserve entropy discretely. Moreover, the attempts on entropy control rely on an imprecise artificial dissipation mechanism which does not guarantee the physical inequality of the entropy. A leap in the advancement of numerical entropy control was made by [Ismail & Roe, 2009] who designed an entropy control flux at an affordable computational cost. In the frame of entropy control, the following definitions of the properties of a numerical scheme are used.

- Entropy Conservation: The entropy variable is conserved with zero entropy production in both space and time.

- Entropy Stability: The entropy generation is captured with the correct sign.
- Entropy Consistency: The entropy generation is captured with the correct sign and amount.

The entropy control numerical scheme in one dimension (1D) described in [Ismail & Roe, 2009] has laid down the foundation for the path towards entropy consistent schemes. In a more recent review paper [Ranocha, 2018], the performances of various entropy stable schemes are tested. It is found that there is no single superior entropy stable scheme over the others. Nevertheless, compared to the schemes without entropy stable feature, these schemes are shown to be more robust and physical in discontinuous cases. Besides, the most of the entropy-conservative fluxes preserves non-negativity of the density variable, which is crucial to produce a stable results.

Although the current literature is rich in entropy control schemes thus far, most of them are in the frame of FVM. Although FVM is conservative by default as mentioned in Section 1.1, it has its own weaknesses relative to RD methods. First and foremost, FVM faces difficulty to simulate multi-dimensional physics accurately as it is designed and extended from solving one-dimensional problem. RD methods are spared from this issue due to its inclusion of multi-dimensional physics in its original design as introduced in [Roe, 1982]. Many researchers also recognize RD methods to be 'genuinely' multi-dimensional [Garcia-Navarro, Hubbard, & Priestly, 1995], [Sidilkover, 1994]. This advantage is more prominent in the presence of highly distorted grids as there is minimum loss in the order of accuracy for RD schemes while FVM experiences tremendous drop in its order of accuracy to zeroth order or even negative gradient [Chizari & Ismail, 2015].

The second flaw of FVM is the large stencil size required to obtain second or even higher order accuracy. Consequently, high order FVM has to include more values from different cells and is greatly affected with bad quality grid. On the other hand, RD methods are designed to have compact stencil even on second or higher order accurate schemes. Hence, it is deduced that the advantage of RD methods being less sensitive to grid distortions is two fold over FVM, at least for high order accurate schemes. Furthermore, a compact stencil is favourable to parallel computing with less data to be transferred between the computation blocks and thus resulting in a more efficient scheme.

The development of entropy control RD schemes is still not fully matured. One of the most advanced entropy-stable RD methods developed is based on the recently found flux-difference RD approach [Ismail & Chizari, 2017] for scalar equations and also Euler equations in [Chizari, 2016]. Some fundamental properties of the method were established and validated with adequate numerical experiments on equilateral grids and the scheme has shown much potential. However, very little is known about the properties of the flux difference RD methods in terms of stability, accuracy preservation, positivity and others on irregular grids. These interesting aspects should be addressed before venturing into the more complicated system of equations.

In the context of Shallow Water Equations (SWE), the entropy function coincides with the energy of the fluid and hence entropy control is also deemed as energy control. The entropy terms can be simply replaced by energy and entropy generation is analogous to energy dissipation when the system undergoes an irreversible process. One interesting feature of SWE is the presence of numerous types of physical source

terms where these were not considered in previous entropy or energy control for different system of hyperbolic conservation laws. The applications of SWE often extend to complex and non-smooth geometries. In the macro scale, it is common for hydrologists to estimate fluid flows around estuaries, coastlines and even low ground with various obstacles of different heights in the study of flooding [Bradford & Sanders, 2002; Guo, Chen, Tang, & Guo, 2016]. SWE are also applied to more local problems such as effect of flows around bridge piers, complicated spillway for water flows and others [H.-R. Chung, Hsieh, & Yang, 2011; Ying & Wang, 2010]. Hence, it is vital to consider the performance of SWE numerical schemes on irregular grids.

On another note in the context of unsteady calculations which is highly related to SWE flows, most RD schemes have to opt for implicit techniques to preserve second order of accuracy which require high computational cost. An explicit RD scheme following the work of [Ricchiuto, 2015] entails complex predictor-corrector steps which is also computationally expensive. There is yet any direct explicit RD schemes that preserve second order of accuracy.

The advantages and potentials of entropy control schemes and RD methods are the main motivation of the current research in expanding Flux-Difference type of RD schemes to SWE which also incorporates source terms.

1.3 Research Objective

The objectives of this research are summarized as follows,

1. To develop the Energy-Stable Residual Distribution (ESRD) method on SWE

with the inclusion of source terms on irregular grids.

2. To determine properties of scalar Flux-Difference RD method on grid distortion effect based on analytical study.
3. To assess the performance of ESRD method on both homogeneous and non-homogeneous SWE based on benchmark test cases.

1.4 Scope of the Research

The research encompasses a detailed study on the implementation of a energy-stable RD method on SWE in two dimensions (2D) with the focus on systematic grid variations. The method properties are analysed on scalar equations analytically with corresponding numerical test cases obtained from an in-house code to verify the findings. Different versions of the code are used to produce solutions for the newly proposed method on homogeneous and non-homogeneous SWE which are then compared to other classic RD methods and energy-stable FVM, subsequently validated with the exact solutions obtained from analytical works.

1.5 Thesis Outline

The contents of this thesis is divided into six chapters. Besides providing the background of this research, the first chapter documents the problem statement, objective and the scope of the research. Next, a thorough review on the literature is given in chapter two, with emphasis on Residual Distribution Methods and Entropy Control. It should be highlighted that the notion of entropy-control and energy-control are used interchangeably in the thesis since they are of the same principle mathematically, even

though physically having different meanings. Chapter three records the mathematical analyses on grid skewness variation performed on the new Flux Difference RD approach. Next, the mathematical formulation and the numerical algorithm of ESRD method on SWE are presented in chapter four. The findings from this research are documented in chapter five, accompanied with proper and detailed discussions on the results. Before the end of this thesis, chapter six provides the conclusion and insight from this research, along with potential future works.

CHAPTER TWO

LITERATURE REVIEW

By utilizing the high computing power technologies, CFD has grown to be a reliable tool for various industries in multiple disciplines of engineering such as aerospace, chemical processes, and even medical researches. The main role of CFD is to numerically solve the physical governing equations of the fluid flow which are usually systems of PDEs since closed form solutions are rare for analytical computations.

Undoubtedly, the Navier-Stokes equations are the fundamental cornerstone in describing fluid flow mathematically which hold the three main conservation laws, namely the conservation of mass, momentum and energy. By examining the nature of the fluid flow of interest, the Navier-Stokes can be simplified to reduce the computational cost. One of the popular examples is the reduction of viscous and other source terms which results in Euler equations. This assumption of inviscid flow is acceptable only for flow with negligibly viscous force relative to inertial or pressure forces. Among other assumptions are incompressible flow with negligible change in density, steady flow with no change of fluid property over time as well as the simplified turbulent models of Reynolds-Averaged Navier-Stokes for turbulent flow.

2.1 Shallow Water Equations (SWE)

The shallow water or Saint-Venant equations were derived as a simplified version of Navier-Stokes equations to describe fluid flows in an open channel [Barré de Saint Venant, 1871] with the focus on the fluid surface profile or fluid height, h . This

set of equations have been employed to model water flow in coastal areas, lakes, estuaries, rivers, reservoirs and other open channel flows. Many studies have been performed on the SWEs, both in the context of numerical schemes development and applications such as bore/tidal wave propagation, wave interaction with bathymetry, stationary hydraulic jump, dam break, flooding, tsunami generation and propagation.

The simplification of SWEs is based on the following assumptions.

- The fluid of interest has a free surface or zero surface tension.
- The fluid is shallow where the depth, h , is much smaller than the longitudinal length scale, L .
- The flow is incompressible and the density is independent of the pressure.
- In the case where sediment, salinity and pollution are not considered, density is constant.

With the assumptions taken into account and a series of derivations from Navier-Stokes equations including hydrostatic pressure consideration and depth averaging, the general 2D SWEs can be expressed in a compact form as the following based on Figure 2.1,

$$\mathbf{u}_t + \vec{\nabla} \cdot \vec{\mathbf{f}}(\mathbf{u}) + \mathbf{s}(\mathbf{u}) = 0, \quad (2.1)$$

where the main variables of water height and depth-averaged momentum in both x - and y -direction as

$$\mathbf{u} = \left[h \quad hu \quad hv \right]^T, \quad (2.2)$$

the fluxes as

$$\vec{\mathbf{f}}(\mathbf{u}) = \begin{bmatrix} \mathbf{f}(\mathbf{u}) & \mathbf{g}(\mathbf{u}) \end{bmatrix} = \begin{bmatrix} hu & hv \\ hu^2 + \frac{1}{2}gh^2 & huv \\ huv & hv^2 + \frac{1}{2}gh^2 \end{bmatrix}, \quad (2.3)$$

and $\mathbf{s}(\mathbf{u})$ is the source terms which includes the contributions from various types of mass or momentum sources for the flow which can be represented as

$$\mathbf{s}(\mathbf{u}) = \begin{bmatrix} 0 \\ gh \frac{\partial z_b}{\partial x} \\ gh \frac{\partial z_b}{\partial y} \end{bmatrix}. \quad (2.4)$$

where g is the gravitational field strength and $z_b(x, y)$ is the height of the bottom topography or sometimes referred as bathymetry. It is obvious that the first equation is the conservation of mass, followed by conservation of momentum in both spatial dimensions. It is noted that although the equations are derived based on a 'shallow' fluid assumption, some deep water flow simulations such as dam break problems based on SWE show acceptable results as well.

This study on non-homogeneous SWE only includes the source term due to bottom topography whereas the homogeneous counterpart assumes flat bathymetry. However, there are numerous extensions to the source terms to fulfil different conditions which are not considered at this developing stage and are summarized in the following.

- Presence of rain that constitutes mass source.

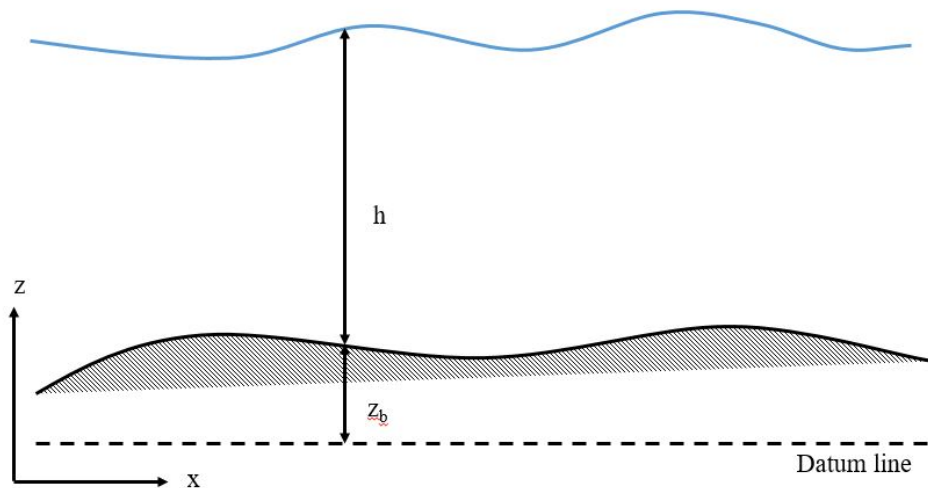


Figure 2.1: Some notations for SWE.

- Infiltration rate, which depicts the rate of mass loss of the fluid that seep through a porous bottom.
- Viscosity of the fluid in the form of second derivative of the velocity along its direction.
- Friction forces from the top and bottom surface of the fluid and its boundary. The top surface is usually associated with wind stress while the bottom friction can be modelled by two families of friction laws based on empirical considerations, namely Manning-Strickler's friction laws as well as laws of Darcy-Weisbach's and Chézy's family.
- Atmospheric pressure gradient which is only apparent with the presence of strong cyclone or typhoon above the fluid surface. Thus, it is dominant in storm-surge forecast.
- Coriolis inertial force, a body force due to the Earth's rotation that causes a relative motion to the fluid.

When the speed of the fluid exceeds certain threshold, the flow characteristics change dramatically where the flow can be classified as subcritical, critical, and supercritical depending on a dimensionless parameter, Froude number (Fr) and defined as

$$\text{Fr} = \frac{u^2 + v^2}{gh}. \quad (2.5)$$

The flow is considered as subcritical or tranquil flow when $\text{Fr} < 1$, critical flow when $\text{Fr} = 1$, and supercritical or rapid flow when $\text{Fr} > 1$. This parameter is analogous to the Mach number in gas dynamics, which is also a ratio of the flow speed to a certain characteristic speed. While this speed is the sound speed for Mach number, it takes the form of wave speed, c while $\text{Fr} = \sqrt{gh}$

Aside from the conventional and well-developed discretization schemes of FDM, FVM and FEM, the RD or Flux Splitting method has also received considerable attention by researchers in SWE over the last three decades due to its special features such as multidimensional upwind [Garcia-Navarro et al., 1995], compact stencil and insensitivity against grid irregularity [Chizari & Ismail, 2015]. In order to ease the discussions in this chapter, the system of SWE are reduced further to scalar equation as

$$\mathbf{u}_t + \vec{\nabla} \cdot \vec{f}(\mathbf{u}) = 0. \quad (2.6)$$

2.2 Finite Volume Method

2.2.1 Overview

Being the most popular choice in CFD software as compared to other methods, FVM is widely believed to be the best option to solve fluid dynamics problems to the

extend some textbooks only mention this particular method when discussing CFD. As mentioned in the previous chapter, FVM first deals with spatial discretization which divides the computational domain of interest into small elements or cells in order to evaluate the integrals of the convective, viscous and even source term fluxes. This spatial splitting process is termed grid generation. According to [Blazek, 2001], there are 3 basic conditions for the division of computational domain.

- the domain is covered by the grid completely,
- there are no empty spaces between the grid cells,
- the grid cells do not overlap each other.

A grid with good quality is also crucial to obtain high quality CFD solution. This is true especially for FVM as it is more sensitive to grid quality relative to the RD method which is described in the following section.

Generally, FVM can be further categorized into cell-centred and cell-vertex schemes based on the positions of the storage for the flow variables and the control volume. The former considers flow quantities to be stored at the centroids of the grid cells which renders the control volumes to be identical to the grid cells. Since this approach is vastly different from RD method, it is not discussed in details here but it is undeniable that cell-centred FVM is way ahead of RD in terms of its development and maturity through the rich literature in terms of investigations on high order schemes and also complicated test cases such as deformable porous media [Lee, Ahn, & Luo, 2018; Nordbotten, 2014; Timothy, Raphaële, & Mario, 2017].

2.2.2 Cell-vertex FVM

To highlight the philosophical difference between Entropy-Stable RD methods and their FVM counterpart, the cell-vertex FVM is revisited since this scheme updates nodal variables, which is more comparable to RD schemes. Since the flow quantities are not stored at the centroids of the cells, the control volumes has to be defined separately from the grid cells. There are different ways to determine the control volumes for cell-vertex FVM such as Voronoi cells, median-dual cells and even staggered cells. The total integration of Equation (2.6) with cell-vertex FVM is performed over the shaded arbitrary Voronoi/containment cell in Figure 2.2(a) using central discretisation. It should be noted that median-dual cell type is used for this study to account for highly skewed cells where the details are included in Appendix A. Voronoi cells are used to illustrate the lack of multi-dimensional property of FVM in a clearer fashion although the same weakness is also present in median-dual cells. The integral is given by

$$\frac{\partial u}{\partial t} = -\frac{1}{A_p} \oint \vec{f}_e \cdot \hat{n}_e dl_e = -\frac{1}{A_p} \sum_e (f_e, g_e) \cdot \vec{n}_e \quad (2.7)$$

$$= -\frac{1}{A_p} \sum_e (f_e n_{e,x} + g_e n_{e,y}), \quad (2.8)$$

where A_p is the Voronoi cell area of point p and subscript e represents quantities at the edges of the Voronoi cells, thus f_e and g_e refer to the flux components across the edge and \vec{n}_e denotes the outwards normal of the edge, \hat{n}_e , scaled by the edge length, l_e . The fluxes across the edges of Voronoi cells are calculated by solving the one-dimensional Riemann problem along the normal direction of the edges. The details in Entropy-Stable FVM computation of the fluxes are recorded in Section 2.4.5.

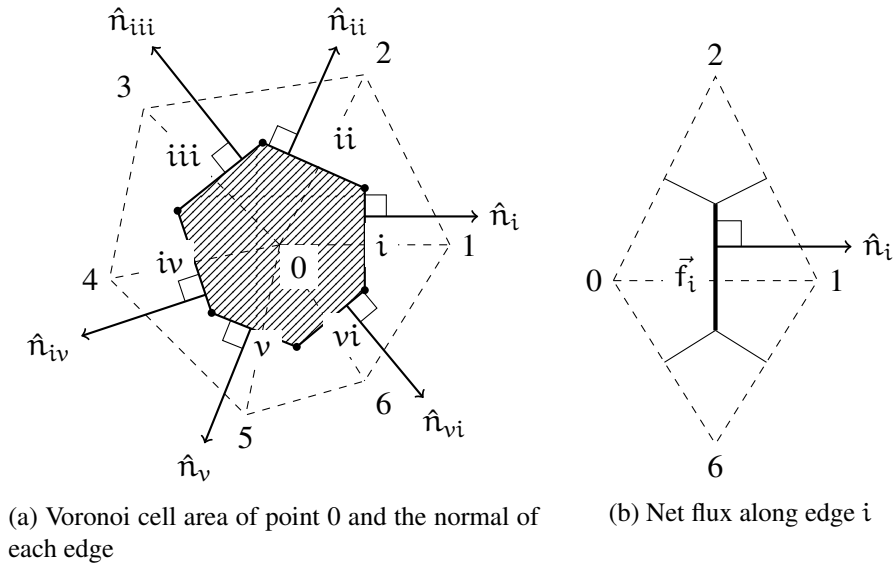


Figure 2.2: The first order finite volume cell vertex diagram.

For first order cell-vertex FVM, the Riemann problem computations on the edge flux are performed by using only the variable values stored in the 2 neighbouring points. It is illustrated in Figure 2.2(b) that the final net flux across edge i is a function of only 2 points on the opposite sides of the edge, which are point 0 and 1. Hence, $\vec{f}_i = \vec{f}(u_0, u_1)$ and it implies that this scheme is not multidimensional.

The second order cell-vertex FVM employs the least square method to reconstruct the variables of each node as polynomials in the Riemann problem computation. In the calculation of node 0 in Figure 2.3, the polynomials of nodes 1 to 6 have to be determined as well. Thus, the computational stencil has to be extended to another layer of cells (in dash lines) for the second order approach. In the consideration of central discretization, the polynomials for point 2 in the same figure has to involve the node variables from point 0, 1, 8, 9, 10, and 3. In another words, second or higher order FVM is unable to have compact stencil since every increment of the order of accuracy has to be accompanied with the inclusion of another layer of cells.

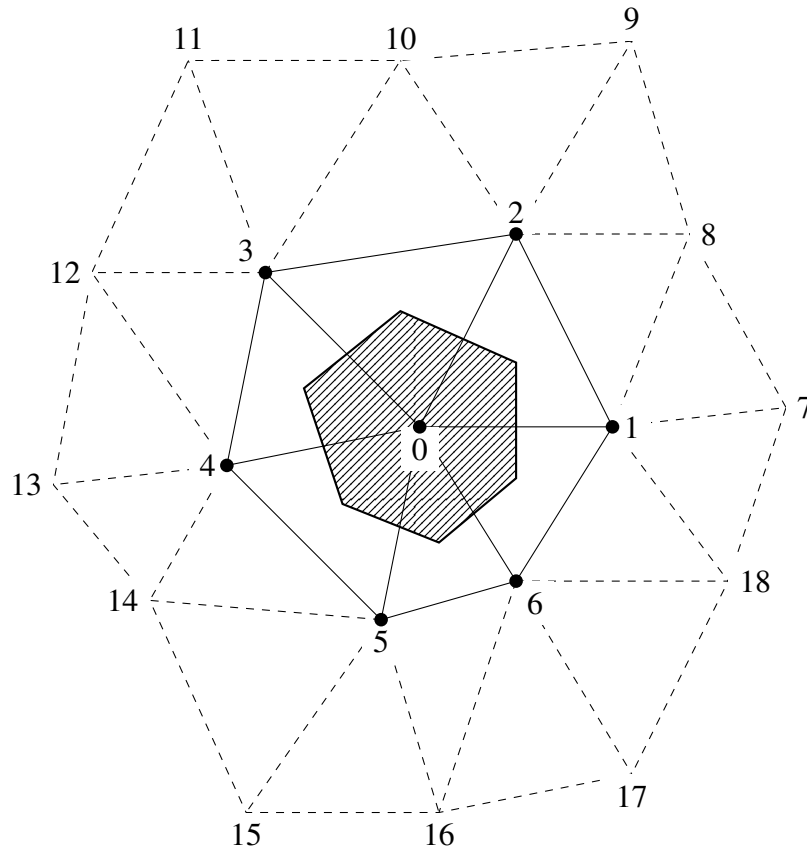


Figure 2.3: The second order finite volume cell vertex stencil diagram.

2.3 Residual Distribution Method

2.3.1 Overview

The concept of RD can be traced back from two distinct research paths back in the 1980s. Hall, Morton and other researchers [Hall, 1986; Morton, Crumpton, & Mackenzie, 1993; Morton, Rudgyard, & Shaw, 1994] worked along the first path concerning the cell-vertex FVM towards an improvement in accuracy. Instead of treating the terms in the PDE separately, the idea of discretizing the residual operator as a whole has shown positive results. The other angle to look at RD method is from the effort of Roe to capture the multidimensional physics of PDE in [Roe, 1982]. Termed as "fluctuation splitting", an Upwind Residual Distribution framework for the 1D Euler equations was proposed from a reconstruction of Roe's flux difference splitting Finite

Volume scheme in that article.

The foundation of RD methods are focused on the implementation of multidimensional physics to tackle the weakness of FVM in retaining one-dimensional physics even for multidimensional problems. Focusing on 2D, a multidimensional upwind model was developed by [Roe, 1986a] for the Euler equations based on simple wave equations instead of the element boundaries, yet without any specific functioning numerical method. Basic differences between RD methods with FVM and FEM were presented in [Deconinck, Ricchiuto, & Lib, 1990] and the significance of RD was established among the CFD community.

The multidimensional upwind model was successfully incorporated with numerical time integration scheme based on the Roe's Riemann solver by [Deconinck, Roe, & Struijs, 1993] where preliminary numerical results were also presented. Hyperbolic and elliptic splitting for RD modelling was introduced by [Mesaros, 1995] and further expanded to preserve flow entropy by [Rad, 2001]. Numerical time integrators of explicit Runge-Kutta and backward implicit were implemented to RD schemes for systems of Euler and Navier-Stokes equations in [van der Weide, 1998]. Moreover, this document includes a good review of the classic RD schemes developed and some parallel computing techniques at that stage.

Struijs in his thesis [Struijs, 1994] provided mathematical proof on the famous Godunov's theorem stating the paradox of having both positivity and linearity preserving properties simultaneously for linear RD schemes. Based on two multidimensional linear RD schemes which are positive and linear preserving individually, [Abgrall,

2001] discussed about a blending approach in an effort to obtain a non-linear scheme that possesses both properties. Extensions to unsteady problem include a construction of second order monotone RD scheme for the Euler equation in [Abgrall & Mezine, 2003].

An algorithm to map RD methods from low order to highest possible order while retaining monotone property was introduced in [Abgrall & Roe, 2003] by tinkering on the degrees of freedom of the element. Mathematical proofs on crucial properties such as consistency, accuracy and convergence were documented in the same article.

High order schemes are often referred to numerical schemes which are third or higher order accurate. Various studies in spatial third order RD method were performed by [Caraeni & Fuchs, 2002] for unsteady Navier-Stokes equations, [Rossiello, 2004] for compressible flow, [Abgrall, Santis, & Ricchiuto, 2014] on conformal meshes. [Rossiello, De Palma, Pascazio, & Napolitano, 2007] further expanded third order accuracy to temporal dimension for RD with quadratic space approximation and third order backward time discretisation. [Mazaheri & Nishikawa, 2015] proposed second and third order accurate RD methods based on Streamline-Upwind Petrov-Galerkin (SUPG) approach.

In the context of RD schemes for system of SWE, [Garcia-Navarro et al., 1995] has first explored the advantage of using multidimensional RD scheme to simulate SWE problems. Due to the very limited application of SWE in steady cases, most numerical schemes of SWE were developed with time-dependent feature even in their early stages. Ricchiuto and other researchers [Hubbard & Ricchiuto, 2011; Ricchiuto,

2015; Ricchiuto, Abgrall, & Deconinck, 2007; Ricchiuto & Bollermann, 2009] have developed a series of conservative RD discretization schemes based on space-time approach, first introduced in [Csík, Ricchiuto, & Deconinck, 2002].

Reviews on developments and future potentials of RD methods are documented and discussed in [Abgrall, 2012; Deconinck et al., 1990] with the references therein.

The general concept of RD methods is described as the following. Starting from the integral form of Equation (2.6) on the grid cells as

$$\iint \left(\mathbf{u}_t + \vec{\nabla} \cdot \vec{f}(\mathbf{u}) \right) dA = 0 \quad (2.9)$$

For steady state computation, the first term vanishes and the remaining term is defined as the total residual or fluctuation in [Roe, 1982]. Hence, the total residual for each element \mathbb{E} is,

$$\phi^{\mathbb{E}} = \iint \vec{\nabla} \cdot \vec{f} dA \quad (2.10)$$

Depending on the different RD schemes used, this total residual is distributed to each node of the cell with the portion defined as

$$\phi_i^{\mathbb{E}} = \zeta_i^{\mathbb{E}} \phi^{\mathbb{E}} \quad (2.11)$$

where ζ_i is the distribution coefficient of node i and by construction, $\sum_{j \in \mathbb{E}} \zeta_j^{\mathbb{E}} = 1$. For each node in the computational domain, it receives some portion of the residual from every cell in the neighbouring set of the node, Ψ as illustrated in Figure 2.4(a). Thus, the integral of Eq. (2.6) is solved over the actual control volume, which is the

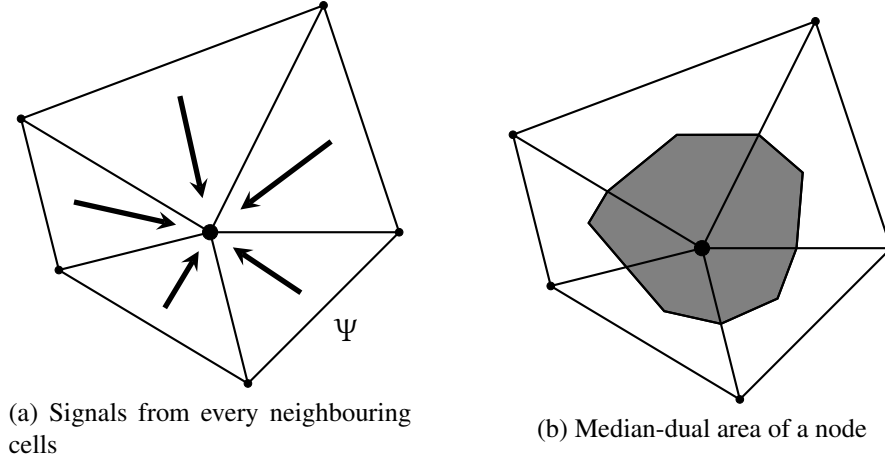


Figure 2.4: Signal directions and median-dual area of a point.

median-dual area as depicted in Fig. 2.4(b).

$$\frac{\partial u_i}{\partial t} + \frac{1}{A_i} \sum_{\mathbb{E} \in \Psi} \phi_i^{\mathbb{E}} = 0 \quad (2.12)$$

where A_i is the median-dual cell area of the node. Based on the semi-discrete form of Equation (2.12), the flow variable u_i can be iterated with proper time discretisation.

2.3.2 Properties of RD Methods

There are generally three common properties of interest within the context of RD methods, namely positivity, linearity preserving and multidimensional upwinding. It should be noted that most of the RD schemes do not inherit all the aforementioned properties but only acquire a subset of those based on the design of each scheme. Godunov Theorem [Godunov, 1959], which is also proven by [Struijs, 1994], states that any linear scheme cannot hold both positivity and linear preserving properties simultaneously. Hence, many research efforts were laid on the design of non-linear schemes such as the Positive Streamwise invariant (PSI) and limited schemes to exhibit both properties together. Each RD property is discussed in the following subsections.

2.3.2(a) Positivity (\mathbb{P})

The presence of discontinuities such as hydraulic jump in SWE context or shock in gas dynamics is rather common in applications and thus inevitable. It is vital for any numerical scheme to capture a monotone shock profile, which can be mathematically presented as positivity to avoid non-physical solutions near the shock region. The constraints of positivity are identical to Local Extremum Diminishing (LED) criterion as described in [Jameson, 1993]. Equation (2.6) is first expressed in semi-discrete form as

$$\left(\frac{\partial \mathbf{u}}{\partial t}\right)_i + \sum_{j \in \Psi} c_{ij}(\mathbf{u}_i - \mathbf{u}_j) = 0, \quad (2.13)$$

and the scheme is deemed positive if

$$c_{ij} \geq 0, \quad \forall i, j, \quad i \neq j. \quad (2.14)$$

Mathematically speaking, this condition is able to ensure that no extrema are generated locally within Ψ but in the same note, does not guarantee that any extrema in the initial condition vanishes over time iterations.

RD schemes that adhere to positivity conditions have low order of accuracy, typically of first order. For flow field without discontinuity, the importance of this property is not apparent and it is more desirable to focus on accuracy.

2.3.2(b) Linearity Preserving (\mathbb{LP})

For fluid problems with steady linear solutions, any numerical scheme is considered to be linear preserving (\mathbb{LP}) if it is able to reproduce exact solutions, which corre-

sponds to the highest possible order of polynomials when the solution over the element has linear variation. Hence, it is also a popular property to be considered in the effort to achieve high order schemes.

There are two ways to interpret $\mathbb{L}\mathbb{P}$ mathematically. The former first considers Equation (2.12) in the form of distribution coefficient, $\zeta_i^{\mathbb{E}}$ and enforcing it to be bounded which can be expressed as

$$\left(\frac{\partial \mathbf{u}}{\partial t}\right)_i + \sum_{\mathbb{E} \in \Psi} \zeta_i^{\mathbb{E}} \phi^{\mathbb{E}} = 0, \quad \zeta_i^{\mathbb{E}} \in [0, 1]. \quad (2.15)$$

The details of this proof can be found in [van der Weide, 1998].

On the other hand, some of the RD schemes cannot be expressed in the form of Equation (2.15) and its inheritance of $\mathbb{L}\mathbb{P}$ property has to be proven with an alternative method. In [Abgrall, 2001], it is shown that a converged RD scheme produces a formally second order accurate solution in steady problem which is based on the first interpretation of $\mathbb{L}\mathbb{P}$ condition. In order to obtain a second order solution, it is deduced that the signals must be of third order accurate, thus $\phi^{\mathbb{E}} = O(l_{\mathbb{E}})^3$ where $l_{\mathbb{E}}$ refers to the grid size.

2.3.2(c) Multidimensional Upwinding (MIU)

An upwinding numerical scheme only allows the flow data to propagate towards the downstream direction. In another words, flow data at a certain point cannot influence the flow variables upstream of that point. In the context of FVM, the flow data or fluxes are computed along the normal of the cell edges and thus the upwind direction